

Research Article

Performance Analysis of the 3GPP-LTE Physical Control Channels

S. J. Thiruvengadam^{1,2} and Louay M. A. Jalloul³

¹ Smart Antenna Research Group, Department of Electrical Engineering, Stanford University, USA

² TIFAC CORE in Wireless Technologies, Thiagarajar College of Engineering, Madurai 625015, India

³ Beceem Communications Inc., Santa Clara, CA 95054, USA

Correspondence should be addressed to Louay M. A. Jalloul, jalloul@beceem.com

Received 8 May 2010; Revised 24 September 2010; Accepted 11 November 2010

Academic Editor: Ashish Pandharipande

Copyright © 2010 S. J. Thiruvengadam and L. M. A. Jalloul. This is an open access article distributed under the Creative Commons Attribution License, which permits unrestricted use, distribution, and reproduction in any medium, provided the original work is properly cited.

Maximum likelihood-based (ML) receiver structures are derived for the decoding of the downlink control channels in the new long-term evolution (LTE) standard based on multiple-input and multiple-output (MIMO) antennas and orthogonal frequency division multiplexing (OFDM). The performance of the proposed receiver structures for the physical control format indicator channel (PCFICH) and the physical hybrid-ARQ indicator channel (PHICH) is analyzed for various fading-channel models and MIMO schemes including space frequency block codes (SFBC). Analytical expressions for the average probability of error are derived for each of these physical channels. The impact of channel-estimation error on the orthogonality of the spreading codes applied to users in a PHICH group is investigated, and an expression for the signal-to-self interference plus noise ratio is derived for Single Input Multiple Output (SIMO) systems. Finally, a matched filter bound on the probability of error for the PHICH in a multipath fading channel is derived. The analytical results are validated against computer simulations.

1. Introduction

A new standard for broadband wireless communications has emerged as an evolution to the Third Generation Partnership Project (3GPP) wideband code-division multiple access (CDMA) Universal Mobile Telecommunication System (UMTS), termed long term evolution or LTE (3GPP-release 8). The main difference between LTE and its predecessors is the use of scalable OFDM (orthogonal frequency division multiplexing, used on the downlink with channel bandwidth of 1.4 all the way up to 20 MHz.) together with MIMO (multiple input multiple output, configurations of up to 4 transmit antennas at the base station and 2 receive antennas at the user equipment.) antenna technology as shown in Table 1. Compared to the use of CDMA in releases 4–7, the LTE system separates users in both the time and frequency domain. OFDM is bandwidth scalable, the symbol structure is resistant to multipath delay spread without the need for equalization, and is more suitable for MIMO transmission and reception. Depending on the antenna configuration, modulation, coding and user category, LTE supports both frequency-division duplexing (FDD) as well

as time-division duplexing (TDD) with peak data rates of 300 Mbps on the downlink and 75 Mbps on the uplink [1–3]. In this paper, the FDD frame structure is analyzed, but the results also reflect the performance of TDD frame structure.

Another fundamental deviation in LTE specification relative to previous standard releases is the control channel design and structure to support the capacity enhancing features such as link adaptation, physical layer hybrid automatic repeat request (ARQ), and MIMO. Correct detection of the control channel is needed before the payload information data can be successfully decoded. Thus, the overall link and system performance are dependent on the successful decoding of these control channels.

The performance of the physical downlink control channels in the typical urban (TU-3 km/h) channel was reported in [4] using computer simulations only, without rigorous mathematical analyses. The motivation behind this paper is to describe the analytical aspects of the performance of optimal receiver principles for the decoding of the LTE physical control channels. We develop and analyze the performance of ML receiver structures for the downlink physical control format indicator channel (PCFICH) as well as the

TABLE 1: System numerology.

Channel bandwidth (MHz) (W)	1.4	3.0	5.0	10.0	15.0	20.0
Number of physical resource blocks (N_{RB}^{DL})	6	15	25	50	75	100
FFT size (N)	128	256	512	1024	1536	1024
Sampling frequency (Mps) (f_s)	1.92	3.84	7.68	15.36	23.04	30.72

physical hybrid ARQ indicator channel (PHICH) in the presence of additive white Gaussian noise, frequency selective fading channel with different transmit and receive antenna configurations, and space-frequency block codes (SFBC). These analyses provide insight into system performance and can be used to study sensitivity to design parameters, for example, channel models and algorithm designs. Further, it would serve as a reference tool for fixed-point computer simulation models that are developed for hardware design.

The rest of the paper is organized as follows. A brief description of the LTE control channel specification is given in Section 2. The BER analyses of the physical channels PCFICH and PHICH are given in Sections 3 and 4, respectively. Section 5 contains some concluding remarks.

Notation. \circ , $*$, and H denote element by element product, complex conjugate, and conjugate transpose, respectively. $\langle \mathbf{x}, \mathbf{y} \rangle = \sum_i x_i y_i^*$ is the inner product of the vectors \mathbf{x} and \mathbf{y} . \otimes denotes the convolution operator.

2. Brief Description of the 3GPP-LTE Standard

The downlink physical channels carry information from the higher layers to the user equipment. The physical downlink shared channel (PDSCH) carries the payload-information data, physical broadcast channel (PBCH) broadcasts cell specific information for the entire cell-coverage area, physical multicast channel (PMCH) is for multicasting and broadcasting information from multiple cells, physical downlink control channel (PDCCH) carries scheduling information, physical control format indicator channel (PCFICH) conveys the number of OFDM symbols used for PDCCH and physical hybrid ARQ indicator Channel (PHICH) transmits the HARQ acknowledgment from the base station (BS). BS in 3GPP-LTE is typically referred to as eNodeB. Downlink control signaling occupies up to 4 OFDM symbols of the first slot of each subframe, followed by data transmission that starts at the next OFDM symbol as the control signaling ends. This enables support for microsleep which provides battery-life savings and reduced buffering and latency [4]. Reference signals transmitted by the BS are used by UE for channel estimation, timing and frequency synchronization, and cell identification.

TABLE 2: Power delay profiles for pedestrian B and ITU channel models.

Ped-B channel model		TU channel model	
Delay (nsec)	Average power (dB)	Delay (μ sec)	Average power (dB)
0	0	0	1.000
200	-0.9	0.813	0.669
800	-4.9	1.626	0.448
1200	-8.0	2.439	0.300
2300	-7.8	3.252	0.200
3700	-23.9	4.056	0.134

The downlink OFDM FDD radio frame of 10 ms duration is equally divided into 10 subframes where each subframe consists of two 0.5 ms slots. Each slot has 7 or 6 OFDM symbols depending on the cyclic prefix (CP) duration. Two CP durations are supported: normal and extended. The entire time-frequency grid is divided into physical resource blocks (PRB), wherein each PRB contains 12 resource elements (subcarriers). PRBs are used to describe the mapping of physical channels to resource elements. Resource element groups (REG) are used for defining the control channels to resource element mapping. The size of the REG varies depending on the OFDM symbol number and antenna configuration [1]. The PCFICH is always mapped into the first OFDM symbol of the first slot of each subframe. For the normal CP duration, the PHICH is also mapped into the first OFDM symbol of the first slot of each subframe. On the other hand, for the extended CP duration, the PHICH is mapped to the first 3 OFDM symbols of the first slot of each subframe. All control channels are organized as symbol-quadruplets before being mapped to a single REG. In the first OFDM symbol, two REGs per PRB are available. In the third OFDM, there are 3 REGs per PRB. In the second OFDM symbol, the number of REGs available per PRB will be 2 for single- or two-transmit antennas, and 3 for four-transmit antennas.

This paper focuses on the performance analyses of the PCFICH and PHICH between the UE and the BS in three types of channels: (1) static (additive white Gaussian noise (AWGN)), (2) frequency flat-fading, and (3) ITU frequency selective channel models. The power-delay profiles of the ITU models, used in the analyses, are given in Table 2.

3. Physical Control Format Indicator Channel

The two CFI bits are encoded using a (32,2) block code as shown in Table 3. The 32 encoded bits are QPSK modulated, layer mapped, and, finally, are resource element mapped.

3.1. PCFICH with SIMO Processing. The received signal is processed as follows: the cyclic prefix is removed, then the FFT is taken, followed by resource-element demapping. The complex-valued output at the k -th receive antenna is modeled as

$$\mathbf{y}_k = \mathbf{h}_k \circ \mathbf{d}^{(n)} + \mathbf{u}_k, \quad k = 1, 2, \dots, K, \quad (1)$$

TABLE 3: CFI (32,2) Block code [2].

CFI	$\langle b_0, b_1, \dots, b_{31} \rangle$
1	$\langle 0, 1, 1, 0, 1, 1, 0, 1, 1, 0, 1, 1, 0, 1, 1, 0, 1, 1, 0, 1, 1, 0, 1, 1, 0, 1, 1, 0, 1, 1, 0, 1, 1, 0, 1 \rangle$
2	$\langle 1, 0, 1, 1, 0, 1, 1, 0, 1, 1, 0, 1, 1, 0, 1, 1, 0, 1, 1, 0, 1, 1, 0, 1, 1, 0, 1, 1, 0, 1, 1, 0, 1, 1, 0 \rangle$
3	$\langle 1, 1, 0, 1, 1, 0, 1, 1, 0, 1, 1, 0, 1, 1, 0, 1, 1, 0, 1, 1, 0, 1, 1, 0, 1, 1, 0, 1, 1, 0, 1, 1, 0, 1, 1 \rangle$
4 (Reserved)	$\langle 0, 0 \rangle$

where K is the number of receive antennas at UE, \mathbf{y}_k is 16×1 received subcarrier vector, $\mathbf{d}^{(n)}$ is the 16×1 complex QPSK symbol vector corresponding to the 32-bit CFI codewords, $1 \leq n \leq 3$, \mathbf{h}_k is 16×1 complex channel frequency response, and \mathbf{u}_k represents the contribution of thermal noise and interference, modeled as zero-mean circularly symmetric complex Gaussian with covariance $E[\mathbf{u}_k \mathbf{u}_k^H] = \sigma_u^2 \mathbf{I}$. Modeling the interference as Gaussian is justified, since in a multicell multisector system such as LTE, there are typically between 3 to 6 dominant interferers. These interferers are uncorrelated due to independent large-scale propagation, short-term fading, and uncorrelated scrambling sequences. Therefore, their sum can be well approximated as a Gaussian random variable. Conditioned on \mathbf{h}_k , \mathbf{y}_k is a complex Gaussian random variable. Maximizing the log-likelihood function of \mathbf{y}_k given \mathbf{h}_k , results in the following ML decision rule:

$$\text{CFI} = \min_{m=1,2,3} \sum_{k=1}^K \left| \mathbf{y}_k - (\mathbf{h}_k \circ \mathbf{d}^{(m)}) \right|^2, \quad (2)$$

which simplifies to

$$\text{CFI} = \arg \max_{m=1,2,3} z^{(m)}, \quad (3)$$

where the soft outputs are given by

$$z^{(m)} = \sum_{k=1}^K z_k^{(m)} \quad \text{for } m = 1, 2, 3, \quad (4)$$

where $z_k^{(m)} = \text{Re}\{\langle \mathbf{y}_k \circ \mathbf{h}_k^*, \mathbf{d}^{(m)} \rangle\}$ for $m = 1, 2, 3$. Expanding (4) yields

$$z^{(m)} = \sum_{k=1}^K \text{Re} \left\{ \sum_{i=1}^{16} (|h_{i,k}|^2 c(1, m) + u_{i,k} d_i^{(m)*} h_{i,k}^*) \right\}, \quad (5)$$

$m = 1, 2, 3,$

where $c(n, m) = \sum_{i=1}^{16} d_i^{(n)} d_i^{(m)*}$. Without loss of generality, it is assumed that the first CFI codeword is used, that is $n = 1$, thus we have

$$c(1, m) = \sum_{i=1}^{16} (d_i^{(1)} d_i^{(m)*}) = \begin{cases} 16 & \text{if } m = 1 \\ -6 - j10 & \text{if } m = 2 \\ -5 + j11 & \text{if } m = 3 \end{cases} \quad (6)$$

as per the predefined CFI codewords in [1]. Then, the probability of error is well approximated by the union bound as

$$\begin{aligned} P_b^{(\text{CFI})} &\leq \sum_{m=2}^3 P(z^{(1)} < z^{(m)} \mid n = 1) \\ &= \sum_{m=2}^3 P(z^{(1)} - z^{(m)} < 0 \mid n = 1), \end{aligned} \quad (7)$$

where $P(z^{(1)} - z^{(m)} < 0 \mid n = 1)$ is the pair-wise error probability (PEP). In the case of a static AWGN channel with $h_{i,k} = h$, $\forall i, k$, and single-receive antenna, let $x = z_1^{(1)} - z_1^{(2)}$ and $y = z_1^{(1)} - z_1^{(3)}$. Thus, x is Gaussian with mean $22|h|^2$ and variance $22\sigma_u^2|h|^2$ and y is Gaussian with mean $21|h|^2$ and variance $21\sigma_u^2|h|^2$. Thus, the union bound can be evaluated to be

$$P_b^{(\text{CFI})} \leq \frac{1}{2} \text{erfc} \left(\sqrt{\frac{11|h|^2}{\sigma_u^2}} \right) + \frac{1}{2} \text{erfc} \left(\sqrt{\frac{10.5|h|^2}{\sigma_u^2}} \right). \quad (8)$$

The union bound can be tightened further, by improving the evaluation of the PEP using the joint probability of error due to CFI = 2 and CFI = 3. Then, the union bound becomes

$$\begin{aligned} P_b^{(\text{CFI})} &\leq \frac{1}{2} \text{erfc} \left(\sqrt{\frac{11|h|^2}{\sigma_u^2}} \right) + \frac{1}{2} \text{erfc} \left(\sqrt{\frac{10.5|h|^2}{\sigma_u^2}} \right) \\ &\quad - \frac{1}{4} \text{erfc} \left(\sqrt{\frac{11|h|^2}{\sigma_u^2}} \right) \text{erfc} \left(\sqrt{\frac{10.5|h|^2}{\sigma_u^2}} \right). \end{aligned} \quad (9)$$

Using the bound that $\text{erfc}(x) \leq \exp(-x^2)$, the joint probability term can be written as,

$$\frac{1}{4} \text{erfc} \left(\sqrt{\frac{11|h|^2}{\sigma_u^2}} \right) \text{erfc} \left(\sqrt{\frac{10.5|h|^2}{\sigma_u^2}} \right) \leq \frac{1}{4} \exp \left(-\frac{21.5|h|^2}{\sigma_u^2} \right). \quad (10)$$

For flat-fading channels, the average pair-wise probability of error, averaged over the channel $|h|^2$ distribution, is given by

$$\overline{P_b^{(\text{CFI})}} = E_{|h|^2} [P_b^{(\text{CFI})}]. \quad (11)$$

For a Rayleigh fading channel, (11) reduces to [5]

$$\overline{P_{b,\text{flat}}^{(\text{CFI})}} \leq \sum_{i=1}^2 \left[\frac{(1-\mu_i)}{2} \right] \sum_{k=0}^{K-1} \binom{K-1+k}{k} \left[\frac{(1+\mu_i)}{2} \right]^k - P_{b3,\text{flat}}^{\text{CFI}}, \quad (12)$$

where $P_{b3,\text{flat}}^{\text{CFI}}$ is evaluated to be

$$P_{b3,\text{flat}}^{\text{CFI}} = \frac{1}{2^{2K+1}(K-1)!(1+\bar{\gamma})^K} \sum_{k=0}^{K-1} b_k (K-1+k)! \left(\frac{\bar{\gamma}}{1+\bar{\gamma}} \right)^k, \quad (13)$$

where $b_k = \sum_{n=0}^{K-1-k} \binom{2K-1}{n}$, $\bar{\gamma} = 21.5\gamma$, $\mu_i = \sqrt{s_i\gamma/(1+s_i\gamma)}$, and $\gamma = 1/\sigma_u^2$ is the SNR per tone per antenna and the scaling factors $s_1 = 11$ and $s_2 = 10.5$.

3.2. Analysis of CFI with Repetition Coding. In this section, we compare the performance of the (32,2) block code of Table 3 used for CFI encoding with a simple rate 1/16 repetition code. The repetition code for CFI = 1 is represented by a 32-bit-length vector [0 1 ··· 0 1], CFI = 2 by [1 0 ··· 1 0], and CFI = 3 by [1 1 ··· 1 1]. When CFI = 1 or CFI = 2, the Hamming distance between the other codewords are 32 and 16, otherwise, the Hamming distance is 16. Since the CFI assumes the value between 1 and 3, in an equiprobable manner, the probability of error, in the static AWGN channel, is given by

$$P_{b,\text{repetition}}^{(\text{CFI})} \leq \frac{1}{3} \operatorname{erfc} \left(\sqrt{\frac{16|h|^2}{\sigma_u^2}} \right) + \frac{2}{3} \operatorname{erfc} \left(\sqrt{\frac{8|h|^2}{\sigma_u^2}} \right). \quad (14)$$

The expression in (14) is compared to that in (9).

3.3. PCFICH with Transmit Diversity Processing. Transmit diversity with two-transmit antennas or four-transmit antennas, is achieved using space frequency block code (SFBC) in combination with layer mapping [1]. Assume that there are two transmit antennas at the BS transmitter and K receive antennas at the UE. The received signal is processed as follows. The output at the l th layer (two consecutive tones), is given by

$$\mathbf{y}_{l,k} = \mathbf{H}_{l,k} \mathbf{d}_l^{(n)} + \mathbf{u}_{l,k} \quad 0 \leq l \leq M_{\text{symp}}^{\text{layer}} - 1, \quad 1 \leq k \leq K, \quad (15)$$

where $M_{\text{symp}}^{\text{layer}} = M_{\text{symp}}/2 = 8$, $\mathbf{y}_{l,k}$ is a 2×1 received-signal vector at the k th receive antenna for the l th layer, $\mathbf{d}_l^{(n)}$ is 2×1 transmit signal vector corresponds to n , where $1 \leq n \leq 3$, at the l th layer, and $\mathbf{u}_{l,k}$ denotes 2×1 thermal-noise vector. The channel matrix $\mathbf{H}_{l,k}$ is given by

$$\mathbf{H}_{l,k} = \frac{1}{\sqrt{2}} \begin{bmatrix} h_{k,1}^{(l)} & -h_{k,2}^{(l)} \\ h_{k,2}^{(l)*} & h_{k,1}^{(l)*} \end{bmatrix}, \quad (16)$$

$h_{k,m}^{(l)}$ is the complex channel frequency response between m th transmit antenna and k th receive antenna, at l th symbol layer. The maximal ratio combiner (MRC) output is given as

$$\mathbf{z}_{l,k} = \mathbf{H}_{l,k}^H \mathbf{y}_{l,k} \quad 0 \leq l \leq M_{\text{symp}}^{\text{layer}} - 1, \quad 1 \leq k \leq K. \quad (17)$$

The decision on the CFI is taken as in (3), and the soft output variable $z^{(m)}$ is given by

$$z^{(m)} = \sum_{k=1}^K \tilde{z}_k^{(m)} \quad \text{for } m = 1, 2, 3, \quad (18)$$

where $z_k^{(m)} = \operatorname{Re} \{ \langle \mathbf{y}_k \circ \mathbf{h}_k^*, \mathbf{d}^{(m)} \rangle \}$, $m = 1, 2, 3$.

For flat-fading channel, $\mathbf{H}_{l,k} = \mathbf{H}_k = (1/\sqrt{2}) \begin{bmatrix} h_{k,1} & -h_{k,2} \\ h_{k,2}^* & h_{k,1}^* \end{bmatrix}$. Then (18) becomes,

$$z^{(m)} = \sum_{k=1}^K \operatorname{Re} \left(\sum_{l=0}^{M_{\text{symp}}^{\text{layer}}-1} \mathbf{H}_k^H \mathbf{H}_k c(1, m) + \sum_{l=0}^{M_{\text{symp}}^{\text{layer}}-1} \langle \mathbf{H}_k^H \mathbf{u}_{l,k}, \mathbf{d}_l^{(m)} \rangle \right) \quad \text{for } m = 1, 2, 3. \quad (19)$$

Without loss of generality, it is assumed that the first CFI codeword is used, that is $n = 1$, where

$$c(1, m) = \sum_{l=0}^{M_{\text{symp}}^{\text{layer}}-1} \langle \mathbf{d}_l^{(1)}, \mathbf{d}_l^{(m)} \rangle = \begin{cases} 16 & \text{if } m = 1 \\ -6 - j10 & \text{if } m = 2 \\ -5 + j11 & \text{if } m = 3 \end{cases}. \quad (20)$$

Substituting for \mathbf{H}_k in (19), it becomes

$$z^{(m)} = \sum_{k=1}^K \left(\frac{\operatorname{Re} \{ c(1, m) \}}{2} (|h_{k,1}|^2 + |h_{k,2}|^2) + \operatorname{Re} \left\{ \sum_{l=0}^{M_{\text{symp}}^{\text{layer}}-1} \langle \mathbf{H}_k^H \mathbf{u}_{l,k}, \mathbf{d}_l^{(m)} \rangle \right\} \right), \quad m = 1, 2, 3. \quad (21)$$

Conditioned on \mathbf{H}_k , $z^{(m)}$ is Gaussian with mean $\sum_{k=1}^K (\operatorname{Re} \{ c(1, m) \} / 2) (|h_{k,1}|^2 + |h_{k,2}|^2)$ and variance $4\sigma_u^2 \sum_{k=1}^K (|h_{k,1}|^2 + |h_{k,2}|^2)$. The probability of error is well approximated by the union bound, as shown in (10).

In the case of single-receive antenna, let $x = z_1^{(2)} - z_1^{(1)}$ and $y = z_1^{(3)} - z_1^{(1)}$. x is Gaussian with mean $11(|h_{k,1}|^2 + |h_{k,2}|^2)$ and variance $11\sigma_u^2(|h_{k,1}|^2 + |h_{k,2}|^2)$ and y is Gaussian with mean $10.5(|h_{k,1}|^2 + |h_{k,2}|^2)$ and variance $10.5\sigma_u^2(|h_{k,1}|^2 + |h_{k,2}|^2)$. In the static AWGN channel, conditioned on $|h|$, the

union bound is evaluated to be

$$P_b^{(\text{CFI})} \leq \frac{1}{2} \operatorname{erfc} \left(\sqrt{\frac{11|h|^2}{\sigma_u^2}} \right) + \frac{1}{2} \operatorname{erfc} \left(\sqrt{\frac{10.5|h|^2}{\sigma_u^2}} \right) - \frac{1}{4} \operatorname{erfc} \left(\sqrt{\frac{11|h|^2}{\sigma_u^2}} \right) \operatorname{erfc} \left(\sqrt{\frac{10.5|h|^2}{\sigma_u^2}} \right). \quad (22)$$

For the MISO flat-fading channel, the average probability of error, averaged over the channel $|h|^2$ distribution, is given by (13) with $\mu_i = \sqrt{0.5s_i\gamma/(1+0.5s_i\gamma)}$. For MIMO (2×2) flat-fading channel, the diversity order $L = 4$ and the average probability of error is given by

$$\overline{P_b^{(\text{CFI})}} \leq \sum_{i=1}^2 \left[\frac{(1-\mu_i)}{2} \right] \sum_{k=0}^{L-1} \binom{L-1+k}{k} \left[\frac{(1+\mu_i)}{2} \right]^k - P_{b3,\text{flat}}^{\text{CFI}}, \quad (23)$$

where

$$P_{b3,\text{flat}}^{\text{CFI}} = \frac{1}{2^{2L+1}(L-1)!(1+\bar{\gamma})^L} \sum_{k=0}^{L-1} b_k (L-1+k)! \left(\frac{\bar{\gamma}}{1+\bar{\gamma}} \right)^k, \quad (24)$$

where $b_k = \sum_{n=0}^{L-1-k} \binom{2L-1}{n}$.

The PCFICH performance in the presence of AWGN is shown in Figure 1. It is seen that the Union Bound approximation closely matches with the Monte Carlo simulation results. It is observed that the predefined codes for CFI yields approximately 0.5 dB SNR improvement compared to a repetition code, at the block-error rate (BLER) of 10^{-2} .

Currently, the fourth CFI codeword in Table 3 is reserved for future expansion. When all the four codewords are used to convey the CFI, an additional term is introduced in the error probability given as $(1/2) \operatorname{erfc}(\sqrt{10.5|h|^2/\sigma_u^2})$ and the Union Bound becomes

$$P_b^{(\text{CFI})} \leq \frac{1}{2} \operatorname{erfc} \left(\sqrt{\frac{11|h|^2}{\sigma_u^2}} \right) + \operatorname{erfc} \left(\sqrt{\frac{10.5|h|^2}{\sigma_u^2}} \right). \quad (25)$$

Thus, it requires an additional 0.45 dB (approximately) to achieve the BLER of 10^{-2} , compared to using the first three codewords. The PCFICH performance in the presence of Rayleigh fading channels is shown in Figure 2.

4. Physical Hybrid ARQ Indicator Channel

The PHICH carries physical hybrid ARQ ACK/NAK indicator (HI). Data arrives to the coding unit in form of indicators for HARQ acknowledgement. Figure 3 shows the PHICH transport channel and physical channel processing on hybrid ARQ data, \mathbf{w}_n is the spreading code for n th user in a PHICH group, obtained from an orthogonal set of codes [1]. In LTE,

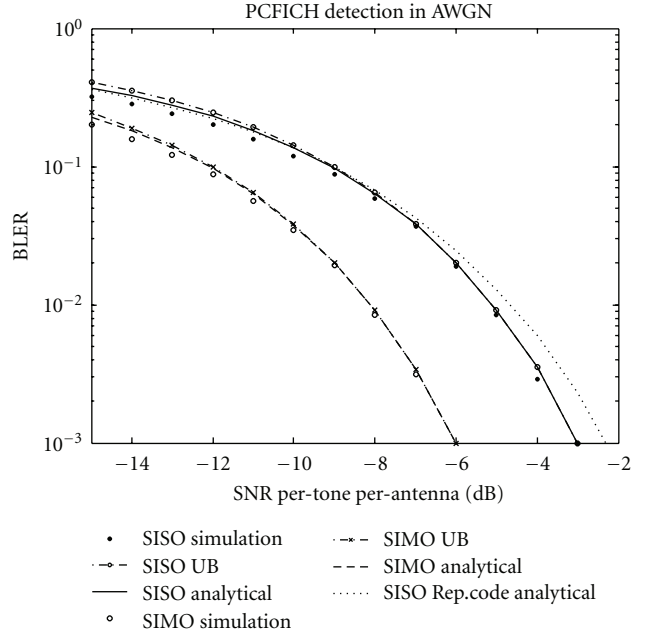


FIGURE 1: PCFICH performance in AWGN.

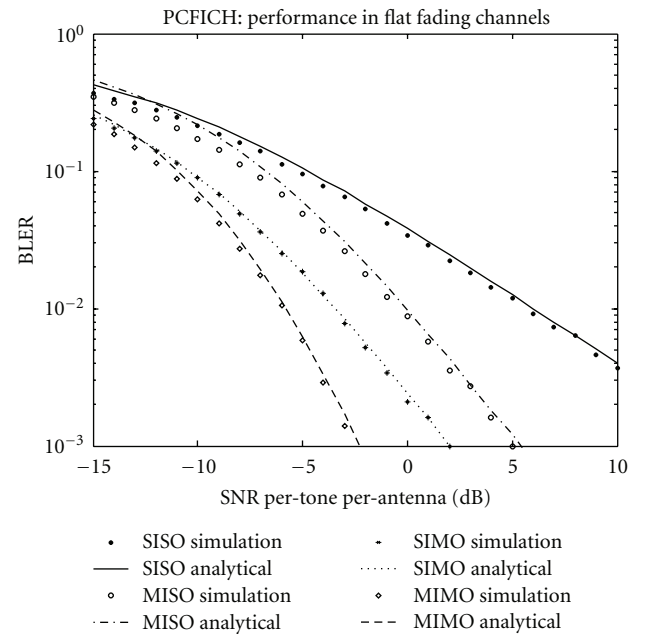


FIGURE 2: PCFICH performance in flat-fading channel.

$2M$ spreading sequences are used in a PHICH group, where $M = 4$ for normal CP and 2 for extended CP. The first set of M spreading sequences are formed by $M \times M$ Hadamard matrix, and the second set of M spreading sequences are in quadrature to the first set.

4.1. PHICH with SIMO Processing. The received signal is processed as follows. The cyclic prefix is removed, then the FFT is taken, followed by resource element demapping. The

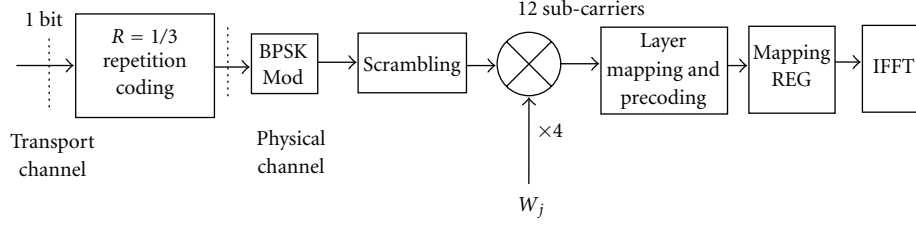


FIGURE 3: PHICH transmit processing.

output that represents the i th resource-element group and k th receiver antenna is given by

$$\mathbf{y}_{i,k} = \mathbf{h}_{i,k} \circ \left(x_1 \sqrt{\frac{P_1}{2}} \mathbf{w}_1 + \sum_{n=2}^M \sqrt{\frac{P_n}{2}} \mathbf{w}_n x_n + j \sum_{n=1}^M \sqrt{\frac{\tilde{P}_n}{2}} \mathbf{w}_n \tilde{x}_n \right) + \mathbf{u}_{i,k}, \quad i = 1, 2, 3. \quad (26)$$

where $\mathbf{y}_{i,k}$ is an $M \times 1$ vector, P_n and \tilde{P}_n , $n = 1, \dots, M$ are the power levels of the M orthogonal codes (for the normal CP case), $x_n \in \{1, -1\}$ is the data bit value of the n th user HI, and x_n and $\mathbf{h}_{i,k}$ is an $M \times 1$ complex channel frequency response vector. Without loss of generality, it is assumed that the desired HI channel to be decoded uses the first orthogonal code denoted as \mathbf{w}_1 . The second and third terms in (26) denote the remaining $2M - 1$ spreading codes used for the other HI channels within a PHICH group (in this analytical model, we treat the general case of the normal CP. The extended CP is easily handled as shown in the final error-rate formulas.) The term $\mathbf{u}_{i,k}$ denotes the thermal noise, which is modeled as circularly symmetric zero-mean complex Gaussian with covariance $E[\mathbf{u}_{i,k} \mathbf{u}_{i,k}^H] = \sigma_u^2 \mathbf{I}$.

The ML decoding is given by

$$\mathbf{z} = \sum_{k=1}^K \mathbf{z}_k, \quad (27)$$

where K is the number of antennas at the UE receiver and

$$\mathbf{z}_k = \sum_{i=1}^3 \mathbf{z}_{i,k}, \quad (28)$$

where

$$\mathbf{z}_{i,k} = \text{Re} \left\{ \left\langle \mathbf{y}_{i,k} \circ \hat{\mathbf{h}}_{i,k}^*, \mathbf{w}_1 \right\rangle \right\}, \quad (29)$$

where the estimated channel frequency response $\hat{\mathbf{h}}_{i,k}$ is given by $\hat{\mathbf{h}}_{i,k} = \mathbf{h}_{i,k} + \mathbf{e}_{i,k}$, $\mathbf{e}_{i,k}$ is the estimation error which is

uncorrelated with $\mathbf{h}_{i,k}$ and zero-mean complex Gaussian with covariance $\sigma_e^2 \mathbf{I}$. By expanding (29), we get that

$$\begin{aligned} z_{i,k} = \text{Re} \left(\left\langle \mathbf{h}_{i,k} \circ \hat{\mathbf{h}}_{i,k}^* \circ \mathbf{w}_1, \mathbf{w}_1 \right\rangle x_1 \sqrt{\frac{P_1}{2}} \right. \\ \left. + \sum_{n=2}^M \left\langle \mathbf{h}_{i,k} \circ \hat{\mathbf{h}}_{i,k}^* \circ \mathbf{w}_n, \mathbf{w}_1 \right\rangle \sqrt{\frac{P_n}{2}} x_n \right. \\ \left. + j \sum_{n=1}^M \left\langle \mathbf{h}_{i,k} \circ \hat{\mathbf{h}}_{i,k}^* \circ \mathbf{w}_n, \mathbf{w}_1 \right\rangle \sqrt{\frac{\tilde{P}_n}{2}} \tilde{x}_n \right. \\ \left. + \left\langle \mathbf{u}_{i,k} \circ \hat{\mathbf{h}}_{i,k}^*, \mathbf{w}_1 \right\rangle \right). \quad (30) \end{aligned}$$

Note that $\langle \mathbf{w}_i, \mathbf{w}_j \rangle = \begin{cases} M, & i=j \\ 0, & i \neq j \end{cases}$. Thus (28) becomes

$$\begin{aligned} z_k = \sum_{i=1}^3 \sum_{m=1}^M \left| h_{i,k}^{(m)} \right|^2 \sqrt{\frac{P_1}{2}} x_1 + \text{Re} \left(\sum_{i=1}^3 \sum_{m=1}^M h_{i,k}^{(m)} e_{i,k}^{(m)*} \right) \sqrt{\frac{P_1}{2}} x_1 \\ - \text{Im} \left(\sum_{i=1}^3 \sum_{m=1}^M h_{i,k}^{(m)} e_{i,k}^{(m)*} \right) \sqrt{\frac{\tilde{P}_1}{2}} \tilde{x}_1 \\ + \text{Re} \left(\sum_{i=1}^3 \sum_{m=1}^M h_{i,k}^{(m)*} u_{i,k}^{(m)} \right) + \text{Re} \left(\sum_{i=1}^3 \sum_{m=1}^M e_{i,k}^{(m)*} u_{i,k}^{(m)} \right), \quad (31) \end{aligned}$$

For ideal channel estimation, then due to the orthogonality property of the spreading codes, no interference is introduced to \mathbf{w}_1 from the other HI channels within a PHICH group. However, in the presence of channel-estimation error, self-interference and cochannel interference are introduced as seen in the second and third terms, respectively, in (31). Since $|\tilde{x}_1|^2 = 1$ and $|x_1|^2 = 1$, the signal to interference plus noise ratio (SINR) of the decision statistic z is thus given by

$$\gamma_z^{\text{non-idealCE}} = \sum_{k=1}^K \frac{P_1 \left(\left(\sum_{i=1}^3 \sum_{m=1}^M \left| h_{i,k}^{(m)} \right|^2 \right)^2 \right)}{\left(\sigma_e^2 (P_1 + \tilde{P}_1) / 2 \right) \left(\sum_{i=1}^3 \sum_{m=1}^M \left| h_{i,k}^{(m)} \right|^2 \right) + \sigma_u^2 \sum_{i=1}^3 \sum_{m=1}^M \left| h_{i,k}^{(m)} \right|^2 + 3M \sigma_u^2 \sigma_e^2}. \quad (32)$$

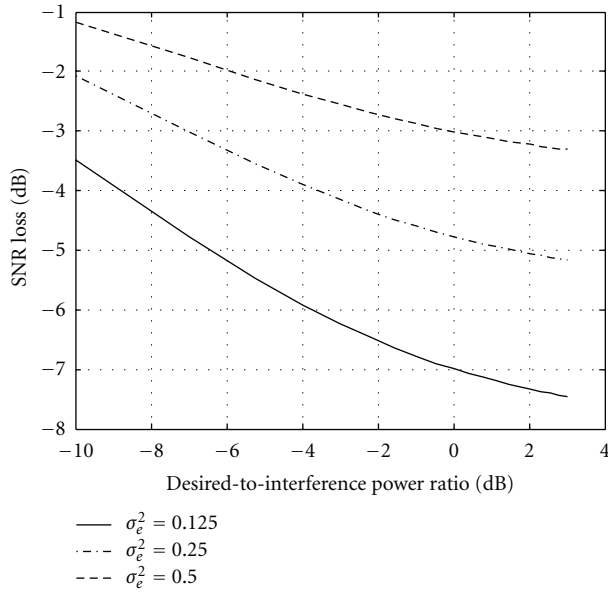


FIGURE 4: Effect of channel estimation error in PHICH.

In the case of a static AWGN channel with a single antenna at the UE receiver, that is, $h_{i,k}^{(m)} = h, \forall i, m, k$, the SINR is simply given by

$$\gamma_z^{\text{non-idealCE}} = \frac{P_G P_1 |h|^4}{0.5 \sigma_e^2 (P_1 + \tilde{P}_1) |h|^2 + \sigma_u^2 |h|^2 + \sigma_u^2 \sigma_e^2}, \quad (33)$$

where $P_G = 12$ in (33) is the processing gain obtained from the spreading code of length 4, and (3,1) repetition code in the case of normal CP [1, 2]. In case of extended CP, a maximum of 4 HI channels are allowed in a PHICH group, and hence a spreading code of length 2 is used for each HI channel, which results in $P_G = 6$.

For ideal channel estimation, $\sigma_e^2 = 0$ and the SNR of the decision statistic z is thus given by

$$\gamma_z^{\text{idealCE}} = \frac{P_G P_1 |h|^2}{\sigma_u^2}. \quad (34)$$

The average loss in SNR due to channel-estimation error is given by

$$L = 1 - \frac{\gamma_z^{\text{non-idealCE}}}{\gamma_z^{\text{idealCE}}} = 1 - \frac{1}{0.5 (\sigma_e^2 / \sigma_u^2) (P_1 + \tilde{P}_1) + 1 + \sigma_e^2}. \quad (35)$$

L is plotted in Figure 4 as a function of the ratio between the desired power to the interfering signal power (P_1 / \tilde{P}_1), for $\sigma_e^2 / \sigma_u^2 = -3$ dB, $\sigma_e^2 / \sigma_u^2 = -6$ dB, and $\sigma_e^2 / \sigma_u^2 = -9$ dB. Figure 4 shows that if $P_1 = \tilde{P}_1$, that is, 0 dB, with $\sigma_e^2 = 0.5 \sigma_u^2$, results in a 3 dB loss in the SNR.

The probability of error in the AWGN case with a single-receive antenna is simply $P_b^{(\text{HI})} = (1/2)P(z < 0 | \text{HI} = 0) + (1/2)P(z > 0 | \text{HI} = 1) = (1/2) \text{erfc}(\sqrt{P_G \gamma})$, γ is the per tone

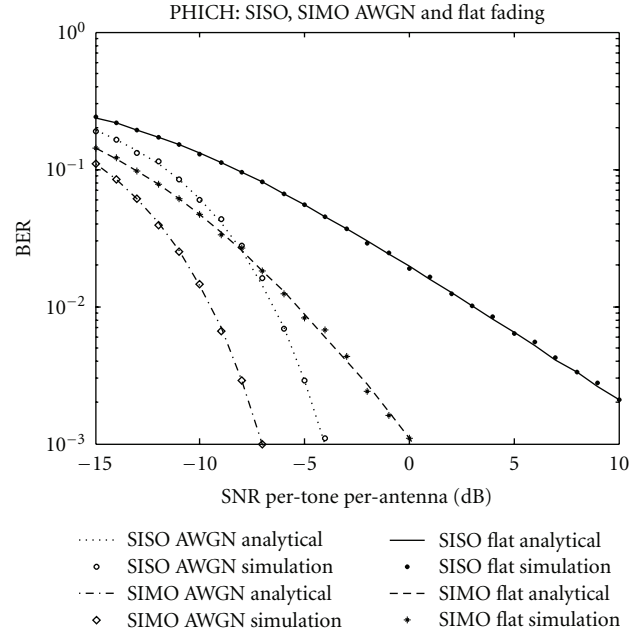


FIGURE 5: PHICH performance in SISO and SIMO systems.

per antenna SNR as shown in (33) and (34). The probability of error averaged over the channel realization is given by

$$\overline{P_b^{(\text{HI})}} = E_\beta [P_b^{(\text{HI})}], \quad (36)$$

where $\beta = \sum_{i=1}^3 \sum_{m=1}^4 |h_{i,k}^{(m)}|^2$. For a frequency-flat Rayleigh fading channel, (36) reduces to [5]

$$\overline{P_b^{(\text{HI})}} = \left[\frac{(1-\mu)}{2} \right]^K \sum_{k=0}^{K-1} \binom{K-1}{k} \left[\frac{(1+\mu)}{2} \right]^k, \quad (37)$$

where $\mu = \sqrt{P_G \gamma / (1 + P_G \gamma)}$.

The PHICH performance for static AWGN and frequency-flat Rayleigh fading channels is shown in Figure 5, for ideal channel estimation.

4.2. PHICH with Transmit Diversity Processing. The received signal is processed as follows. The cyclic prefix is removed, then the FFT is taken, followed by resource-element demapping. The output at the l th layer (consecutive two tones) on the k th receive antenna and i th resource element group (REG) is given by

$$\mathbf{y}_{l,k}^{(i)} = \mathbf{H}_{l,k}^{(i)} \mathbf{d}_l^{(i)} + \mathbf{u}_{l,k}^{(i)} \quad 0 \leq l \leq M_{\text{symp}}^{\text{layer}} - 1, \quad 1 \leq k \leq K, \quad i = 1, 2, 3, \quad (38)$$

where $M_{\text{symp}}^{\text{layer}} = M_{\text{symp}} / (3 \times 2) = 2$, $\mathbf{y}_{l,k}^{(i)}$ is a 2×1 received-signal vector, $\mathbf{d}_l^{(i)}$ is 2×1 transmit-signal vector, and $\mathbf{u}_{l,k}^{(i)}$ denotes 2×1 thermal-noise vector, and each of its elements is modeled as circularly symmetric zero-mean complex Gaussian with covariance $E[\mathbf{u}_{l,k}^{(i)} \mathbf{u}_{l,k}^{(i)H}] = \sigma_u^2 \mathbf{I}$. The channel

matrix $\mathbf{H}_{l,k}^{(i)}$ is given by

$$\mathbf{H}_{l,k}^{(i)} = \frac{1}{\sqrt{2}} \begin{bmatrix} h_{k,1}^{(l)(i)} & -h_{k,2}^{(l)(i)} \\ h_{k,2}^{(l)(i)*} & h_{k,1}^{(l)(i)*} \end{bmatrix}, \quad (39)$$

where $h_{k,m}^{(l)(i)}$ is a complex channel-frequency response between m th transmit antenna and k th receive antenna, at l th symbol layer in i th REG. The transmit-signal vector $\mathbf{d}^{(i)}$ is generated by layer mapping and precoding the HI data vector \mathbf{x} in i th REG. The 4×1 vector \mathbf{x} is given by

$$\mathbf{x} = x_1 \sqrt{\frac{P_1}{2}} \mathbf{w}_1 + \sum_{n=2}^M \sqrt{\frac{P_n}{2}} \mathbf{w}_n x_n + j \sum_{n=1}^M \sqrt{\frac{\tilde{P}_n}{2}} \mathbf{w}_n \tilde{x}_n. \quad (40)$$

P_n and \tilde{P}_n $n = 1, 2, 3, 4$ are the power levels of the 8 spreading codes. The soft output from each layer is given by

$$\mathbf{z}_{l,k}^{(i)} = \mathbf{H}_{l,k}^{(i)H} \mathbf{y}_{l,k}^{(i)} \quad 0 \leq l \leq M_{\text{symp}}^{\text{layer}} - 1, \quad 1 \leq k \leq K, \quad (41)$$

$i = 1, 2, 3.$

The ML decision statistic, is given by

$$z = \sum_{k=1}^K \tilde{z}_k, \quad (42)$$

where

$$\tilde{z}_k = \sum_{i=1}^3 \tilde{z}_k^{(i)} = \sum_{i=1}^3 \text{Re} \left(\sum_{l=0}^{M_{\text{symp}}^{\text{layer}} - 1} \langle \mathbf{z}_{l,k}^{(i)}, \mathbf{w}_1 \rangle \right), \quad (43)$$

and where

$$\mathbf{z}_{l,k}^{(i)} = \mathbf{H}_{l,k}^{(i)H} \mathbf{H}_{l,k}^{(i)} \mathbf{d}_l^{(i)} + \mathbf{H}_{l,k}^{(i)H} \mathbf{u}_{l,k}^{(i)} \quad 0 \leq l \leq M_{\text{symp}}^{\text{layer}} - 1, \quad (44)$$

$1 \leq k \leq K, \quad i = 1, 2, 3.$

In a flat-fading channel, $\mathbf{H}_{l,k}^{(i)} = \mathbf{H}_k \forall l, i$. Then the decision statistic z is given by,

$$z = \sum_{k=1}^K \sum_{i=1}^3 \left(\mathbf{H}_k^H \mathbf{H}_k \sum_{l=0}^{M_{\text{symp}}^{\text{layer}} - 1} \text{Re}(\langle \mathbf{d}_l^{(i)}, \mathbf{w}_1 \rangle) + \sum_{l=0}^{M_{\text{symp}}^{\text{layer}} - 1} \text{Re}(\langle \mathbf{H}_k^H \mathbf{u}_{l,k}^{(i)}, \mathbf{w}_1 \rangle) \right). \quad (45)$$

The instantaneous SNR of z is evaluated to be

$$\text{SNR}_z = \sum_{k=1}^K \frac{6P_1 (|h_{k,1}|^2 + |h_{k,2}|^2)}{\sigma_u^2}. \quad (46)$$

In the case of a static AWGN channel with a single antenna at the UE receiver, that is, $h_{i,k} = h, \forall i, k$, the SNR is given by $\text{SNR}_z = |h|^2 (12P_1/\sigma_u^2)$. The probability of error is given by,

$$P_b^{(\text{HI})} = \frac{1}{2} \text{erfc}(\sqrt{P_G \gamma}). \quad (47)$$

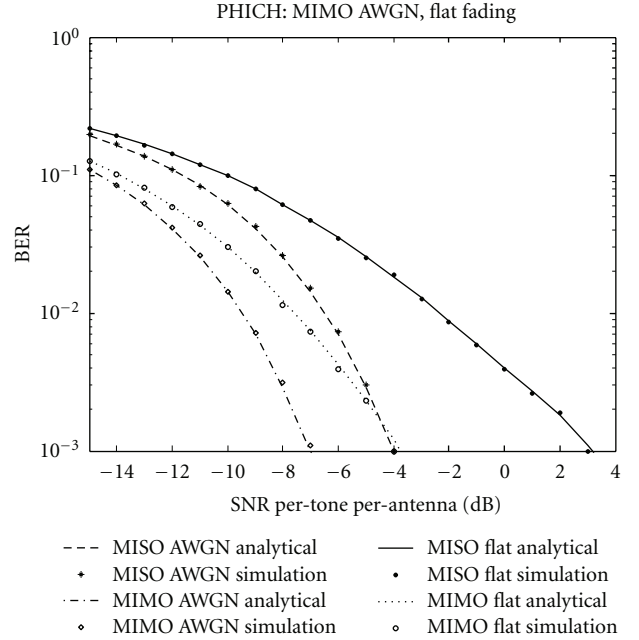


FIGURE 6: PHICH performance in MIMO systems.

For the MISO Rayleigh flat-fading channel, the average probability of error, averaged over the channel $|h|^2$ distribution, is given by [5]

$$P_b^{(\text{HI})} = \left[\frac{(1 - \mu_f)}{2} \right]^{K-1} \sum_{k=0}^{K-1} \binom{K-1+k}{k} \left[\frac{(1 + \mu_f)}{2} \right]^k, \quad (48)$$

where $\mu_f = \sqrt{0.5P_G \gamma_k / (1 + 0.5P_G \gamma_k)}$ and $\gamma_k = P_1/\sigma_u^2$, is the SNR per antenna.

For a MIMO (2×2) flat-fading channel, the average probability of error is given by

$$P_b^{(\text{HI})} = \left[\frac{(1 - \mu_f)}{2} \right]^{L-1} \sum_{k=0}^{L-1} \binom{L-1+k}{k} \left[\frac{(1 + \mu_f)}{2} \right]^k, \quad (49)$$

where the diversity order $L = 4$.

Figure 6 shows the PHICH performance in MIMO systems in the presence of AWGN and Rayleigh flat-fading channels. The analytical results match well with the computer simulations.

4.3. Matched Filter Bound for ITU Channel Models. The objective of this section is to analyze the performance of the LTE downlink control channel PHICH, in general, using matched filter bounds for various practical channel models. The base band channel impulse response can be represented as

$$\tilde{h}(t) = g(t) \otimes \sum_{i=1}^p \alpha_i z_i \delta(t - \tau_i) = \sum_{i=1}^p \alpha_i z_i g(t - \tau_i), \quad (50)$$

where α_i and τ_i are the amplitude and delay of the i th path which define power delay profile (PDP), z_i is a zero-mean,

unit-variance complex Gaussian random variable, $g(t) = \sin(2\pi Wt)/\pi t$, and W is the system bandwidth. Let $\tilde{\mathbf{h}}$ be a $N \times 1$ complex vector that contains N_R nonzero taps which depends on the sampling frequency, and its corresponding system bandwidth is as shown in Table 1. The channel frequency response is given by,

$$h(k) = G(k) \sum_{m \in \mathbf{T}} \alpha_m z_m e^{-j(2\pi/N)mk} \quad k = 0, 1, \dots, N-1, \quad (51)$$

where \mathbf{T} is $N_R \times 1$ tap-locations vector of $\tilde{\mathbf{h}}$ at which the tap coefficient is nonzero.

The decision statistic SNR or matched filter bound (MFB) of PHICH is a function of $\beta = \sum_{k=1}^K \sum_{i=1}^3 \sum_{m=1}^4 |h_{i,k}^{(m)}|^2 = \mathbf{h}_e \mathbf{h}_e^H$, where $\mathbf{h}_e = [h_{1,1}^{(1)} \dots h_{1,1}^{(4)} \dots h_{3,1}^{(1)} \dots h_{3,1}^{(4)} h_{1,2}^{(1)} \dots h_{3,2}^{(4)} \dots h_{1,K}^{(1)} \dots h_{3,K}^{(4)}]$. Thus, the MFB is a function of $12K$ independent chi-square distributed random variables with 2 degrees of freedom. For single-receive antenna

$$\beta = \sum_{p=1}^{12} \sum_{n=1}^{N_R} \lambda_{p,n} x_{p,n}, \quad (52)$$

where $x_{p,n}$ is independent chi-square distributed random variable with 2 degrees of freedom and $\lambda_{p,n}$ is the average power of p th element of \mathbf{h}_e . Since $\lambda_{p,n}$ is constant with respect to p for the given PDP, MFB can be simply written as

$$\beta = 12 \sum_{n=1}^{N_R} \lambda_n x_n. \quad (53)$$

The characteristics function of β is given by

$$E(e^{i\nu\beta}) = \prod_{n=1}^{N_R} \frac{1}{1 - j\nu\lambda_n}. \quad (54)$$

As λ_n 's are distinct, the probability density function is given by

$$p(\beta) = \sum_{n=1}^{N_R} k_n \frac{e^{-\beta/\lambda_n}}{\lambda_n}, \quad (55)$$

where $k_n = \prod_{j=1, j \neq n}^{N_R} (1/(1 - (\lambda_j/\lambda_n)))$. Then, the bit-error probability for the matched-filter outputs is given by $P_e(\gamma | \beta) = (1/2) \operatorname{erfc}(\sqrt{\gamma\beta})$ [5]. The average probability of error, $P_e = \int_0^\infty P_e(\gamma | \beta) p(\beta) d\beta$ is given by

$$P_e = \sum_{n=1}^{N_R} \frac{k_n}{2} \left(1 - \sqrt{\frac{12\lambda_n\gamma}{1 + 12\lambda_n\gamma}} \right). \quad (56)$$

In case of transmit diversity using SFBC, MFB of PHICH is the function of $\beta = \sum_{k=1}^K \sum_{m=1}^2 \sum_{i=1}^3 \sum_{l=1}^{M_{\text{syimb}}^{\text{layer}}} |h_{i,k}^{(l)(m)}|^2$. For a MIMO system, the channels are assumed to be independent and have the same statistical behavior [7]. For single-receive antenna, the MFB is a function of 12 independent chi-square distributed random variables with 2 degrees of freedom, and it is written as $\beta = 12 \sum_{n=1}^{N_R} \lambda_n x_n$ as in (54).

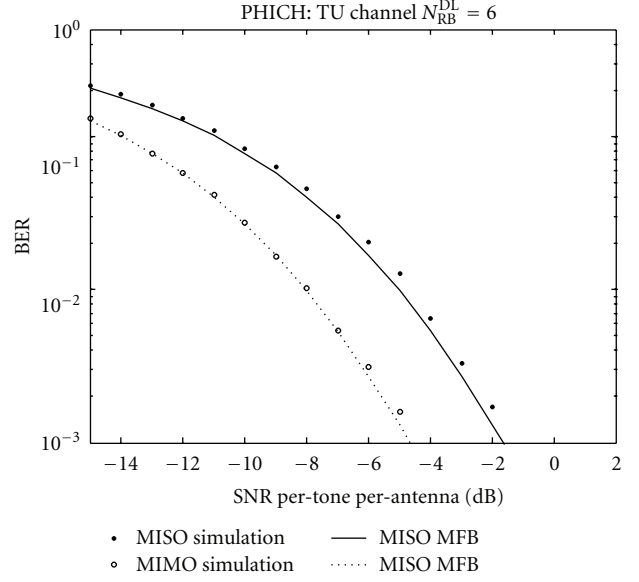


FIGURE 7: PHICH performance in TU channel.

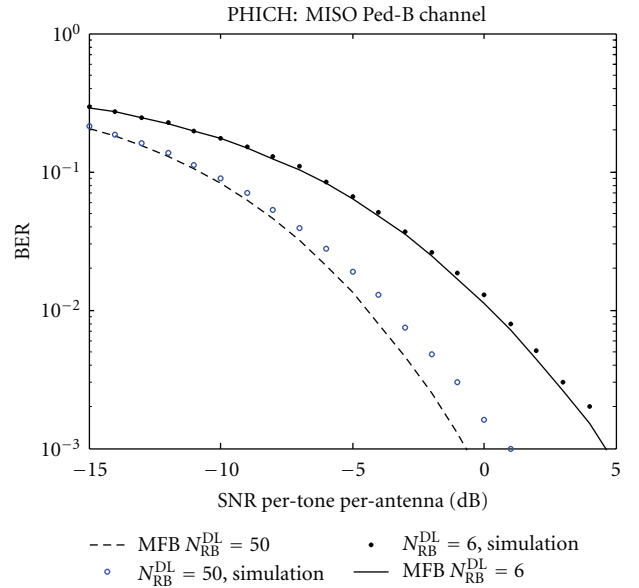


FIGURE 8: PHICH performance in Ped-B channel.

It is observed that in TU channel, all the six paths are resolvable for the system bandwidths specified in Table 1, and in a Ped-B channel, only 4 paths are resolvable for $N_{\text{RB}}^{\text{DL}} = 6$, corresponds to the system bandwidth of 1.4 MHz, where $N_{\text{RB}}^{\text{DL}}$ is the number of PRBs used for downlink transmission. For $N_{\text{RB}}^{\text{DL}} = 6$, the average powers of resolvable taps of each channel coefficient are $[0.1883, 0.1849, 0.1197, 0.1806, 0.1131, 0.1741]$ for a TU channel and $[0.3298, 0.0643, 0.0673, 0.0017]$ for a Ped-B channel. The average powers of resolvable taps for $N_{\text{RB}}^{\text{DL}} = 50$, and in a Ped-B channel are $[0.4057, 0.3665, 0.1269, 0.0663, 0.0688, 0.0017]$. The performances of PHICH for a TU channel with $N_{\text{RB}}^{\text{DL}} = 6$

for MISO and MIMO systems and a Ped-B channel with $N_{RB}^{DL} = 50$ and $N_{RB}^{DL} = 6$ are shown in Figures 7 and 8, respectively. It is also observed that the performance of Ped-B channels at $N_{RB}^{DL} = 50$ has approximately 4.7 dB SNR gain with $N_{RB}^{DL} = 6$, at the BER of 10^{-3} , and a TU channel has 3 dB SNR gain.

5. Conclusion

In this paper, the performance of maximum-likelihood-method-based receiver structures for PCFICH and PHICH was evaluated for different types of fading channels and antenna configurations. The effect of channel-estimation error on the orthogonality of spreading codes used in a PHICH group was studied. These analytical results provide a bound on the channel-estimation-error variance and thus, ultimately decide the channel-estimation algorithm and parameters needed to meet such a performance bound.

References

- [1] 3GPP TS 36.211, "Evolved Universal Terrestrial Radio Access (E-UTRA); Physical Channels and Modulation (Release 8)".
- [2] 3GPP TS 36.212, "Evolved Universal Terrestrial Radio Access (E-UTRA); Multiplexing and Channel Coding (Release 8)".
- [3] 3GPP TS 36.306, "Evolved Universal Terrestrial Radio Access (E-UTRA); User Equipment (UE) radio access capabilities (Release 8)".
- [4] R. Love, R. Kuchibhotla, A. Ghosh et al., "Downlink control channel design for 3GPP LTE," in *Proceedings of IEEE Wireless Communications and Networking Conference (WCNC '08)*, pp. 813–818, Las Vegas, Nev, USA, April 2008.
- [5] J. Proakis, *Digital Communications*, McGraw-Hill, Boston, Mass, USA, 3rd edition, 1995.
- [6] F. Ling, "Matched filter-bound for time-discrete multipath Rayleigh fading channels," *IEEE Transactions on Communications*, vol. 43, no. 2, pp. 710–713, 1995.
- [7] A. F. Naguib, "On the matched filter bound of transmit diversity techniques," in *Proceedings of the International Conference on Communications (ICC '01)*, pp. 596–603, Helsinki, Finland, June 2000.